Colloids and Surfaces B: Biointerfaces 208 (2021) 112138

Contents lists available at ScienceDirect

Colloids and Surfaces B: Biointerfaces

journal homepage: www.elsevier.com/locate/colsurfb

Protocols

Non-specific adsorption of protein to microfluidic materials

Sabaa Rashid [a,d], Jesse Ward-Bond [a,d], Oleksiy Krupin [b,d], Pierre Berini [b,c,d,*]

[a] Department of Chemical and Biological Engineering, University of Ottawa, Ontario, Canada
[b] School of Electrical Engineering and Computer Science, University of Ottawa, Ontario, Canada
[c] Department of Physics, University of Ottawa, Ontario, Canada
[d] Centre for Research in Photonics, University of Ottawa, Ontario, Canada

ARTICLE INFO

Keywords:
Non-specific adsorption
Biofouling
Biosensing
Surface characterization
CYTOP

ABSTRACT

Non-specific adsorption of proteins to the surfaces of microfluidic channels poses a serious problem in lab-on-a-chip devices involving complex biological fluids. Materials commonly used in the formation of microfluidic channels include CYTOP, silica and SU-8. CYTOP is a transparent fluoropolymer (Poly[perfluoro(4-vinyloxy-1-butene)]) with a low refractive index that approximately matches the refractive index of biologically compatible fluids, and is useful in optical biosensors. Using a microfluidic and fluorescence microscopy set-up, the non-specific adsorption of bovine serum albumin (BSA) labeled with fluorescein isothiocyanate (FITC) to three grades of CYTOP (S, M and A), silica, and SU-8 is investigated. Surface properties such as roughness and wettability are also characterized via an atomic force microscope and a contact angle measurement system. The non-specific adsorption of protein occurs with a highly variable load across these materials. Surprisingly, significantly lower adsorption occurred on SU-8 compared to the other materials, likely due to its hydrophilicity (post-cleaning). Among the 3 grades of CYTOP considered, the lowest adsorption occurred on S-grade. BSA adsorption to silica was higher than on S-grade CYTOP and significantly higher than on SU-8 despite being hydrophilic, due to a fixed positive charge formed within the layer during fabrication, which attracts negatively-charged BSA in buffer.

1. Introduction

The non-specific adsorption (NSA) of protein to the surfaces of microfluidic channels is a serious problem in many lab-on-a-chip devices [1,2], particularly in affinity biosensors involving complex biological fluids (*e.g.*, blood products such as plasma and serum, mucous, nasopharyngeal fluid, urine, etc…) [3]. While biosensing requires specific adsorption of biomolecules to functionalized regions via immobilized bioreceptors such as antibodies or enzymes, proteins inevitably adsorb to un-functionalized regions of microfluidic chips resulting in biofouling. In addition to clogging channels, NSA may mask or falsify results in biosensing by reducing sensitivity and selectivity, by raising detection limits, or by causing cross-contamination between samples.

Minimizing NSA in microfluidics depends in part on knowledge of the protein load that inherently forms on the material chosen to implement the channels and the underlying interaction mechanisms leading to the load. Non-specific protein affinity for a solid surface depends on the protein itself and its amino acid constituents which can be charged depending on the pH of their environment, as well as the size and structural stability of the protein [4]. The surface hydrophobicity, charge, topography, and chemical composition also significantly influence the NSA of proteins, in addition to the external conditions at which experiments are conducted [2,4]. The binding strength could be quantified when studying the NSA of proteins to material surfaces by introducing protein extraction compounds such as sodium dodecyl sulfate (SDS) to indirectly correlate binding strength with the amount of the remained protein onto the surface [5].

Dielectric materials are commonly used in biosensor devices to implement microfluidic channels, or to introduce an insulating layer or an optical cladding in electronic, electrochemical or optical biosensors. Silica and SU-8 are often used for this purpose, and more recently, fluoropolymers. Understanding the NSA of proteins to such materials is fundamental to biosensor device applications.

SU-8 is composed of a polymeric epoxy resin, and a photoinitiator dissolved in gamma-Butyrolactone or cyclopentanone organic solvents, and used as a negative resist for defining structures in lithographic processes upon the exposure to UV light [6]. It has been used in many bioanalytical applications involving microfluidic channels and cell

* Corresponding author at: School of Electrical Engineering and Computer Science, University of Ottawa, Ontario, Canada.
E-mail address: berini@eecs.uottawa.ca (P. Berini).

https://doi.org/10.1016/j.colsurfb.2021.112138
Received 2 October 2020; Received in revised form 22 September 2021; Accepted 23 September 2021
Available online 28 September 2021
0927-7765/© 2021 Elsevier B.V. All rights reserved.

Table 1
CYTOP grades and SU-8 spin parameters on Laurell WS-650-23NPP spin coater.

Substance	Step	Spin Speed (rpm)	Acceleration (rpm/s)	Duration (s)
M-grade CYTOP	1	500	200	3
	2	500	0	10
	3	1000	200	3
	4	1000	0	30
	5	0	-200	6
A-grade CYTOP and S-grade CYTOP	1	1000	200	6
	2	1000	0	10
	3	1500	200	3
	4	1500	0	30
	5	0	-300	5
SU-8 2005	1	1000	200	6
	2	1000	0	10
	3	4000	600	6
	4	4000	0	30
	5	0	-700	6

microculture systems [7], and exhibits poor adhesion of biomolecules to its surface [8].

CYTOP (Poly[perfluoro(4-vinyloxy-1-butene)]) is a transparent fluoropolymer whose properties render it useful for a wide range of applications such as an insulator in organic semiconductors, a protective film coating, and a material for the fabrication of optical fibers [9]. CYTOP is chemically compatible with many organic solvents such as hexane, acetone, and isopropanol. It has a low refractive index, similar to that of water [9], making it interesting for use in optical biosensors, including those based on surface plasmon resonance (SPR) which enable label-free real-time detection [10]. Three types of CYTOP are available commercially, exploiting different terminal groups: M-grade with amide-silane terminal functional group (-CONH-Si$(OR)_n$), A-grade with carboxyl terminal functional group (-COOH), and S-grade with trifluoromethyl terminal group (-CF_3) [9].

CYTOP has been used as a dielectric cladding and to form microfluidic channels in long-range surface plasmon-polariton (LRSPP)-based waveguide biosensors composed of a thin straight gold waveguide [11,12]. Once filled with the sensing fluid, the sensing channels become optically non-invasive because the refractive index of CYTOP is close to that of aqueous sensing solutions. The gold waveguide is functionalized with a self-assembled monolayer (SAM) bound to biological receptors (*e.g.* antibodies) to later enable binding to the analyte (*e.g.* antigen) when introducing a sensing fluid. This biosensor was used to demonstrate protein sensing using bovine serum albumin (BSA) [13], the selective capture of human red blood cells [14], and the detection of leukemia markers using a functionalization strategy involving Protein G and antibodies [3].

Bovine Serum Albumin (BSA) is a globular protein that has a high concentration in physiological fluids [4] and is commonly used to block non-specific interactions between cells and the underlying surface in cell adhesion research [15], or to block un-functionalised adsorption sites in biosensors when working with complex fluids [3]. In addition, BSA is similar to human serum albumin (HSA) in molecular weight, isoelectric point and globular dimensions [16]. Here we use BSA labeled with fluorescein isothiocyanate (FITC) as an NSA indicator, and investigate via fluorescence microscopy the BSA load on different surfaces, particularly, 3 grades of CYTOP (S, M, A), silica and SU-8. We also investigate the topography and wettability of the starting substrates using atomic force microscopy and contact angle microscopy.

2. Materials and methods

2.1. Sample fabrication

M-grade CYTOP (CTL-809M from AGC Chemicals Company) and A-grade CYTOP (CTX-809A from AGC Chemicals Company) were spin-coated on two p-type silicon wafers, 2-in. in diameter then the wafers were placed on a hot plate set to room temperature and ramped up to a temperature of 200 °C where the wafers were left for approximately 18 h. A third 2-in. Si wafer was used to prepare S-grade CYTOP samples, by first spin-coating M-grade, then baking it at 50 °C for 30 min, then spin-coating S-grade CYTOP (CTX-809SP2 from AGC Chemicals Company) on top of the M-grade (S-grade CYTOP adheres poorly to a Si wafer). The wafer was then placed on a hot plate set to room temperature and ramped up to a temperature of 200 °C, then baked for approximately 18 h.

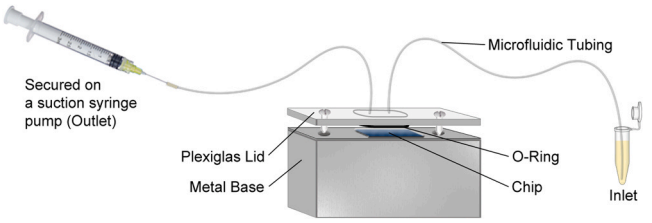

Fig. 1. Schematic diagram of the fluidic jig used for conducting the non-specific adsorption of BSA to different thin films with integrated microfluidic tubings having an outer diameter of 550 μm and inner diameter of 250 μm (IDEX). The BSA and PBS solutions flow from right to left.

SU-8 samples were prepared by spin-coating SU-8 2005 (formally MicroChem, now Kayaku Advanced Materials, Inc.) on another 2-in. Si wafer then subjecting it to a soft-bake of 65 °C for 5 min, followed by 10 min at 95 °C. The SU-8 film was then flood-exposed under UV light with an OAI 200IR mask aligner and an I-Line filter (365 nm bandpass) at 69 mJ/cm^2 exposure energy. Post-exposure, the wafer was then baked at 65 °C for 10 min, removed from the hot plate, and baked for another 20 min at 95 °C. Spin parameters of the 3 grades of CYTOP, along with SU-8 are shown in Table 1.

In addition to the aforementioned films, a 2-in. Si wafer bearing a 100 nm thick layer of thermally grown silica (gate oxide – dense amorphous SiO_2, Carleton University, Ottawa, Canada) was used.

The thicknesses of M-, A- and S-grade CYTOP and SU-8 films were measured to be 1.65, 2.3, 2.5, and 0.68 μm, respectively. CYTOP, silica and SU-8 have refractive indices of about 1.34 [9], 1.46 [17], and 1.59 [18], respectively.

2.2. Solution preparation

Fluorescein isothiocyanate (FITC) labeled bovine serum albumin (BSA) and phosphate buffer saline (PBS) 0.01 M, pH 7.4 were obtained from Sigma-Aldrich. PBS solution was prepared from the package by dissolving it in 1 L of deionized water producing a buffer of the following constitution: 0.01 M phosphate buffer saline, 0.138 M NaCl and 0.0027 M KCl (according to the manufacturer). BSA solution was prepared by mixing the FITC-labeled BSA with PBS to a concentration of 100 μg mL^{-1}.

2.3. Experimental

A custom fluidic jig was used to conduct NSA experiments, composed of a Plexiglas lid with two holes for the inlet and outlet microfluidic tubings, a fluorocarbon O-Ring (Apple Rubber Products Inc.) attached to the bottom of the lid facilitating an effective seal and fluid exchange, and a metal base (Al) to support the chip in a groove and the lid with screws, as shown in Fig. 1.

The wafers (See Section 2.1) were cleaved using a diamond-tipped pen into approximately 6 × 5 mm^2 chips to fit in the groove of the metal base of the custom fluidic jig shown in Fig. 1. The wafers were cleaved rather than diced to avoid re-depositing debris formed while dicing, thus decreasing contamination and surface particulate. The cleaved chips were then washed with distilled/deionized water

Table 2
Summary of the characterization results of each film: Typical fluorescence images obtained over an area of 819 × 819 μm^2, typical AFM scans taken over an area of 20 × 20 μm^2, and water droplet images used for measuring the static contact angle.

Film	Fluorescence Image	AFM Scan	Water Droplet
M-CYTOP	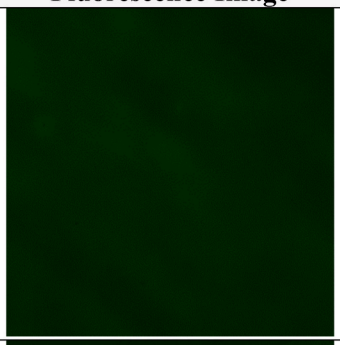	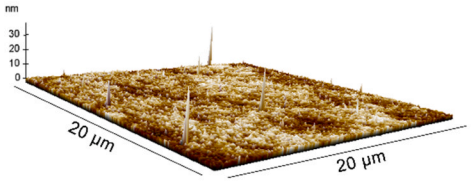	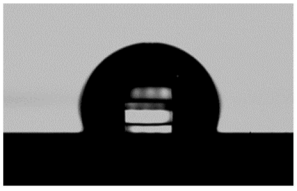
A-CYTOP	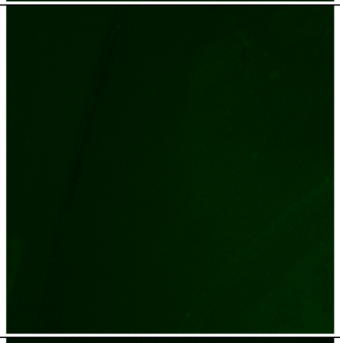	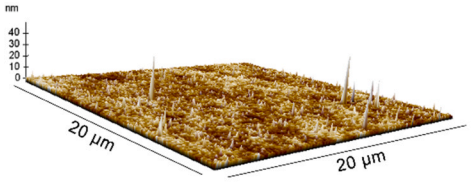	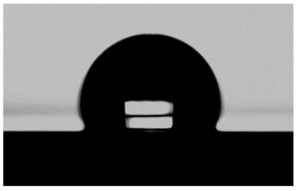
S-CYTOP	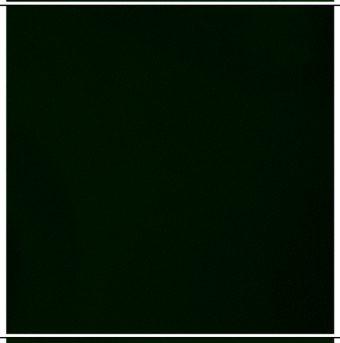	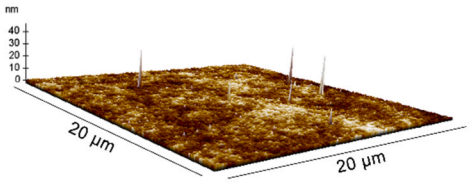	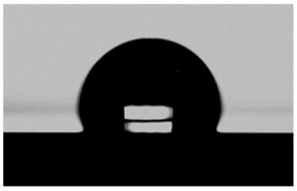
Silica	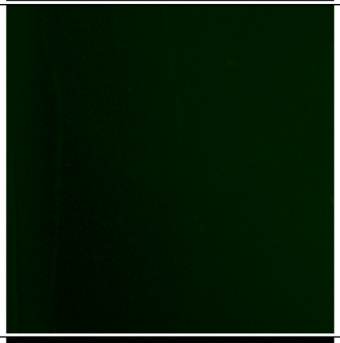	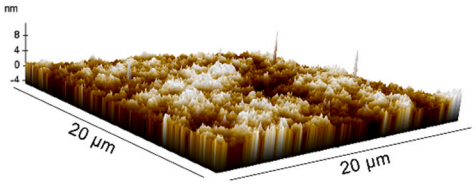	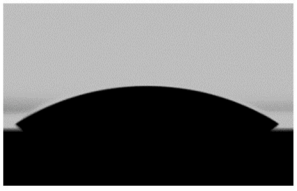
SU-8	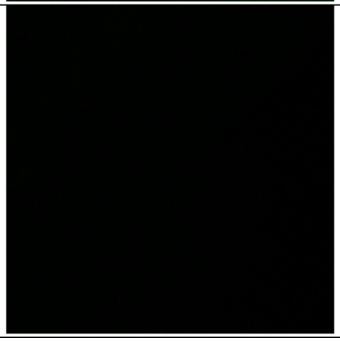	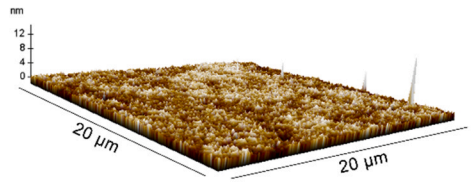	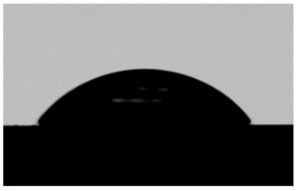

($DDIH_2O$), followed by isopropanol (IPA) wash, dried with nitrogen gas, and placed into a UV/Ozone chamber (Novascan, PSD-UV4) for 15 min with the UV lamp on and an additional 15 min with the UV lamp off to remove any possible organic surface contaminants.

A chip was then placed and secured on the metal base of the fluidic jig (Fig. 1). To prepare the chip and fluidic tubing, IPA in a syringe was manually injected, forming a pressure-driven flow from left to right in the microfluidic channel (Fig. 1), followed by injection of DDI water using a second syringe, and a final injection of PBS using a third syringe. Priming with IPA first was necessary to prevent the trapping of air bubbles since IPA wets the chip and tubing more effectively than water.

The PBS syringe was then secured to a Pico Plus syringe pump (from Harvard Apparatus), set to operate under suction, such that fluids would now be pulled through the microfluidic channel from right to left (Fig. 1), and the PBS syringe used to receive waste. BSA solution in a vial was used as the input fluid and the pump was set to run for 14 min at a flowrate of 30 μL min^{-1}, ensuring complete exchange of fluid in the microfluidic channel and full exposure of its inner surfaces to BSA. The pump was stopped and the pressure was allowed to stabilize in the system before replacing the BSA vial with a vial containing PBS only, in order to rinse the chip and remove any non-adsorbed BSA, by running for 14 min at the same flowrate. The chip was subsequently placed on a microscope slide, covered with a droplet of VectaShield anti-fade mounting medium (Vector Laboratories, H-1000-10), and sealed with a coverslip on top.

The experiment was repeated 3 times on different chips (set 1) for each tested surface. Another set of 3 chips (set 2) was placed on a microscope slide immediately after the UV/Ozone treatment, covered with the anti-fade mounting medium and a coverslip to produce negative-control chips that were not exposed to the BSA solution. The 2 sets of samples were stored in the refrigerator, protected from light, at 4 °C until inspected via fluorescence microscopy.

In Addition, several chips from the same wafers were used for roughness measurement with atomic force microscopy (AFM), and water contact angle measurements shortly after the UV/Ozone exposure.

2.4. Characterization

2.4.1. Fluorescence microscopy

The NSA of FITC-labeled BSA to 3 grades of CYTOP, silica and SU-8 was evaluated through the use of a Nikon Ni-U upright ratiometric fluorescence microscope, using a Nikon Plan Apo objective lens with a magnification of 10 × and a numerical aperture of 0.45. Fluorescence images were captured using an Andor iXon Ultra 897 cooled EMCCD camera. The chips were illuminated using a laser source of wavelength $\lambda_0 = 475$ nm (spectraX), and FITC fluorescence was isolated using 512/45 emission filter (489.5–534.5 nm). The average fluorescence intensity over areas of 819 × 819 μm^2 was calculated as the average of 16-bit pixel intensity values, using NIS-Elements AR software and MATLAB. Three chips that were exposed to BSA were visualized near their center, and 3 other negative-control chips were visualized at several locations (3 measurements per chip) to account for auto-fluorescence on the negative-control chips.

2.4.2. Atomic force microscopy (AFM)

Non-contact-mode AFM roughness images of the chips were obtained using a Park Systems NX10 AFM with a Tap300Al-G tip from NanoAndMore.

2.4.3. Contact angle measurements

Static water contact angle was measured with a VCA Optima System (AST Products Inc.). A 1 μL droplet of DI water was dispensed onto a chip using an integrated micro-syringe. The contact angle was calculated based on placing manual markers surrounding the droplet. Nine measurements were averaged per tested surface. Images of the DI water droplet on the films (found in Table 2) were captured using the camera of the VCA Optima System.

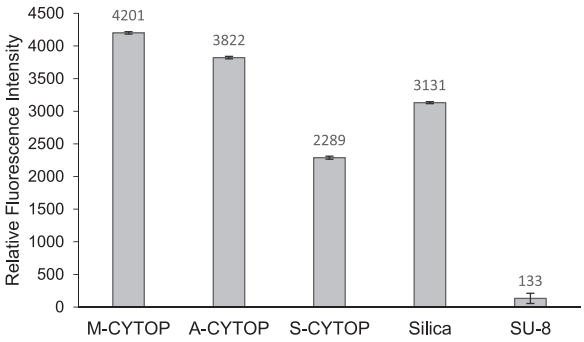

Fig. 2. Comparison of FITC-labeled-BSA adsorption to 3 grades of CYTOP, silica and SU-8 after exposing the surfaces to 100 μg mL^{-1} of fluorescently-labeled BSA by measuring the fluorescence intensity. The data of each bar corresponds to the relative fluorescence intensity, ± 1 standard deviation calculated from 3 positive independent experiments and 9 negative-control measurements.

3. Results and discussion

Fluorescence microscopy was used to test the non-specific adsorption of BSA labeled with FITC to 3 grades of CYTOP, silica and SU-8. The averaged intensity was calculated over 3 chips of each film, corrected by subtracting the averaged intensity calculated over 9 measurements on negative-control samples not exposed to BSA (to account for auto-fluorescence), yielding the relative fluorescence intensity plotted in Fig. 2. It is worth noting that all tested surfaces produced auto-fluorescence measured on negative-control chips but the highest was observed on SU-8 which is consistent with the strong auto-fluorescence reported in the literature for this material [19]. The variance of positive intensities var(P) was added to the variance of the negative-control intensities var(N) to find the standard deviation (σ) as shown in Eq. (1), and represented by the error bars on Fig. 2.

$$\sigma = \sqrt{var(P) + var(N)} \quad (1)$$

The results given in Fig. 2 show that the highest amount of BSA was adsorbed to M-grade CYTOP and the least to S-grade CYTOP among the 3 CYTOP grades. Adsorption to the silica surface was between those observed for A-grade and S-grade CYTOP. Adsorption to SU-8 was significantly lower than for all other substrates. Notably, the small error bars were achieved by optimizing the experimental protocol to that described in Section 2.2 (i.e., introducing the buffer solution prior to introducing the BSA solution after priming with IPA and DI water), in addition to minimizing the surface roughness through careful process control, minimizing debris and contamination by cleaving the wafers into chips rather than dicing, and applying appropriate cleaning steps before commencing the experiments.

To further investigate the results shown in Fig. 2, the surface roughness and wettability were evaluated using an AFM and a contact angle measurement system. Fig. 3(a) reveals sub-1 nm average surface roughness (R_a) values for all films, taken over areas of 20 × 20 μm^2. Ra is low and similar for all films, suggesting that roughness does not play a significant role in the NSA of BSA to the films.

Fig. 3(b) shows the averaged water contact angle measured on each film. The 3 CYTOP grades are hydrophobic since their contact angle is above 90°, whereas silica and SU-8 are hydrophilic since their contact angle is below 90°. SU-8 typically has a water contact angle of approximately 78° [7], which differs significantly from the one measured here (52° ± 2°) due to treatment with UV/Ozone and the formation of hydrophilic functional groups on the SU-8 surface. A previous study showed that a functional group of C═O forms after the

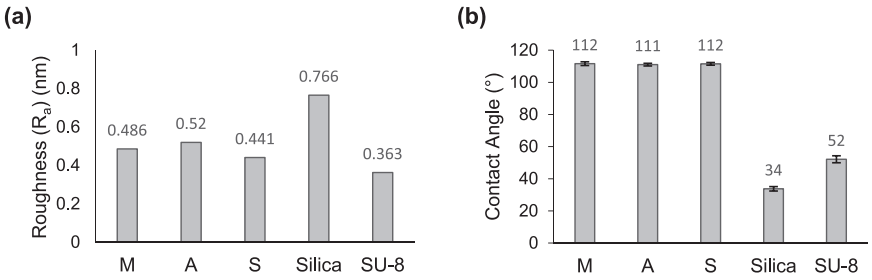

Fig. 3. (a) Sub-1 nm averaged surface roughness (Ra) over an area of 20 × 20 μm^2 measured with an AFM on the M-grade CYTOP, A-grade CYTOP, S-grade CYTOP, silica, and SU-8 films. (b) Water contact angle measured on the same 3 CYTOP grades, silica, and SU-8 films. Measurements show that all CYTOP grades are hydrophobic since their contact angle is above 90°, contrary to silica and SU-8 which are hydrophilic because their contact angle is below 90°.

UV/ozone treatment in addition to the increase of benzene-OH functional group which render SU-8 hydrophilic [7]. A higher BSA load was observed for the hydrophobic films (particularly M- and A-grade CYTOP). This is likely due to the energetically-preferred interaction of ordered water molecules with each other in solution, rather than competing with BSA to adsorb to the hydrophobic film [4]. When protein interacts with the film, the ordered water layer is disturbed in an energetically favorable way, encouraging protein adsorption. S-grade CYTOP exhibited lower adsorption of BSA likely due to its -CF_3 terminal group which limits protein adsorption [20], compared to the amide-silane functional groups in M-grade CYTOP that form strong covalent bonds, and carboxyl functional groups in A-grade CYTOP that form hydrogen bonds [21] upon interaction with proteins. Adsorption of fibronectin on -CF3 was reported the lowest which resulted in reduced cell proliferation when compared to other surface chemistries such as carboxyl and amide groups [20]. This is also consistent with the charge-trapping characteristics of the 3 grades of CYTOP which strongly depend on their terminal group. The order of solid-state electron affinity was found to be S-grade < A-grade < M-grade [22]. Significantly lower BSA was adsorbed to SU-8, possibly due the hydrophilicity of the film on which water molecules compete with protein through the formation of hydrogen bonds. However, this explanation does not apply to the -OH terminated silica film despite its hydrophilicity. Rather, the thermal growth of silica on silicon produces positive trapped charge in the layer [23], resulting in the attraction of protein if the latter is negatively charged, as is the case here with BSA in a buffer at a pH of 7.4 (the isoelectric point of BSA is ~ 4.7) [24].

Table 2 summarizes the results discussed in this section. The second column gives typical fluorescence images taken over an 819 × 819 μm^2 area of FITC-labeled-BSA adsorbed on surfaces of each of the 3 CYTOP grades, silica and SU-8. The next column gives typical AFM scans taken over a 20 × 20 μm^2 area on each tested surface and over which the averaged surface roughness (R_a) was measured. The last column gives example images of a water droplet on each film used in calculating the averaged contact angle.

4. Summary and conclusions

The non-specific adsorption of 100 μg mL^{-1} BSA in PBS to CYTOP (A-, S-, and M-grade), silica and SU-8 films on silicon was investigated through measurements of fluorescence intensity of BSA labeled with FITC. Surface roughness and water contact angle measurements on all films were measured to support the analysis. All surfaces were cleaned using IPA and DI water, then subjected to a UV-Ozone treatment immediately before exposure to the BSA solution. The lowest adsorption occurred on SU-8, likely due to its hydrophilicity. Among the 3 grades of CYTOP considered, the lowest adsorption occurred on S-grade. BSA adsorption to silica was higher than on S-grade CYTOP and SU-8 despite being hydrophilic, due to fixed positive charge trapped in thermally grown silica on silicon and BSA being negatively charged in pH neutral buffer.

CRediT authorship contribution statement

SR and JWB carried out the experiments. SR prepared the first draft of the manuscript. All authors contributed to data interpretation and edited the manuscript. OK and PB directed the project.

Declaration of Competing Interest

The authors declare that they have no known competing financial interests or personal relationships that could have appeared to influence the work reported in this paper.

Acknowledgments

Financial support provided by the Natural Sciences and Engineering Research Council (NSERC) of Canada is gratefully acknowledged. Anthony Olivieri and Howard Northfield are gratefully acknowledged for their assistance. R. Niall Tait and Rob Vandusen are gratefully acknowledged for supplying thermally-grown silica film on silicon wafers.

References

[1] J.Y. Lichtenberg, Y. Ling, S. Kim, Non-specific adsorption reduction methods in biosensing, Sensors 19 (2019) 2488, https://doi.org/10.3390/s19112488.
[2] M. Rabe, D. Verdes, S. Seeger, Understanding protein adsorption phenomena at solid surfaces, Adv. Colloid Interface Sci 162 (2011) 87–106, https://doi.org/10.1016/j.cis.2010.12.007.
[3] O. Krupin, C. Wang, P. Berini, Detection of leukemia markers using long-range surface plasmon waveguides functionalized with Protein G, Lab Chip 15 (2015) 4156–4165, https://doi.org/10.1039/C5LC00940E.
[4] D.A. Puleo, R. Bizios (Eds.), first ed.Biological Interactions on Materials Surfaces Understanding and Controlling Protein, Cell, and Tissue Responses, 20, Springer New York, New York, NY, 2009 https://doi.org/10.1007/978-0-387-98161-1.
[5] V. Sharma, K.A. Blackwood, D. Haddow, L. Hook, C. Mason, J.F. Dye, E. García-Gareta, Method for estimating protein binding capacity of polymeric systems, Biochim. Open 1 (2015) 40–50, https://doi.org/10.1016/j.biopen.2015.10.001.
[6] F. Ceyssens, R. Puers, in: B. Bhushan (Ed.), SU-8 Photoresist BT - Encyclopedia of Nanotechnology, Springer, Netherlands, Dordrecht, 2012, pp. 2530–2543, https://doi.org/10.1007/978-90-481-9751-4_360.
[7] C.-J. Chang, C.-S. Yang, L.-H. Lan, P.-C. Wang, F.-G. Tseng, Fabrication of a SU-8-based polymer-enclosed channel with a penetrating UV/ozone-modified interior surface for electrokinetic separation of proteins, J. Micromech. Microeng. 20 (2010), 115031, https://doi.org/10.1088/0960-1317/20/11/115031.
[8] Y. Wang, J.-H. Pai, H.-H. Lai, C.E. Sims, M. Bachman, G.P. Li, N.L. Allbritton, Surface graft polymerization of SU-8 for bio-MEMS applications, J. Micromech. Microeng. 17 (2007) 1371–1380, https://doi.org/10.1088/0960-1317/17/7/020.
[9] AGC Inc , Chemicals Company-Cytop Technical Brochure, n.d. ⟨http://www.agc.com/kagaku/shinsei/cytop/en/⟩.
[10] D.R. Shankaran, K.V. Gobi, N. Miura, Recent advancements in surface plasmon resonance immunosensors for detection of small molecules of biomedical, food and environmental interest, Sens. Actuators B Chem. 121 (2007) 158–177, https://doi.org/10.1016/j.snb.2006.09.014.
[11] C. Chiu, E. Lisicka-Skrzek, R.N. Tait, P. Berini, Fabrication of surface plasmon waveguides and devices in Cytop with integrated microfluidic channels, J. Vac. Sci. Technol. B 28 (2010) 729–735, https://doi.org/10.1116/1.3449187.
[12] P. Berini, Long-range surface plasmon polaritons, Adv. Opt. Photonics 1 (2009) 484–588, https://doi.org/10.1364/AOP.1.000484.

[13] O. Krupin, H. Asiri, C. Wang, R.N. Tait, P. Berini, Biosensing using straight long-range surface plasmon waveguides, Opt. Express. 21 (2013) 698–709, https://doi.org/10.1364/OE.21.000698.
[14] O. Krupin, C. Wang, P. Berini, Selective capture of human red blood cells based on blood group using long-range surface plasmon waveguides, Biosens. Bioelectron. 53 (2014) 117–122, https://doi.org/10.1016/j.bios.2013.09.051.
[15] P.A. Dimilla, S.M. Albelda, J.A. Quinn, Adsorption and elution of extracellular matrix proteins on non-tissue culture polystyrene petri dishes, J. Colloid Interface Sci. 153 (1992) 212–225, https://doi.org/10.1016/0021-9797(92)90313-B.
[16] T.J. Su, J.R. Lu, R.K. Thomas, Z.F. Cui, J. Penfold, The conformational structure of Bovine Serum Albumin layers adsorbed at the silica–water interface, J. Phys. Chem. B 102 (1998) 8100–8108, https://doi.org/10.1021/jp981239t.
[17] W.A. Pliskin, R.P. Esch, Refractive index of SiO2 films grown on silicon, J. Appl. Phys. 36 (1965) 2011–2013, https://doi.org/10.1063/1.1714393.
[18] A. Borreman, A.M.S. Musa, A. Kok, M.B.J. Diemeer, A. Driessen, Fabrication of polymeric multimode waveguides and devices in SU-8 photoresist using selective polymerization, in: H.F.S. Taco D. Visser, Daan Lenstra (Eds.), Proceedings of the IEEE/LEOS Benelux Chapter 2002 Annual Symposium, Vrije Universiteit Amsterdam, Amsterdam, The Netherlands, 2002, pp. 83–86. ⟨http://doc.utwente.nl/58192/⟩.
[19] J.-H. Pai, Y. Wang, G.T. Salazar, C.E. Sims, M. Bachman, G.P. Li, N.L. Allbritton, Photoresist with low fluorescence for bioanalytical applications, Anal. Chem. 79 (2007) 8774–8780, https://doi.org/10.1021/ac071528q.
[20] G. Altankov, K. Richau, T. Groth, The role of surface zeta potential and substratum chemistry for regulation of dermal fibroblasts interaction, Materwiss. Werksttech. 34 (2003) 1120–1128, https://doi.org/10.1002/mawe.200300699.
[21] Y. Sakane, Y. Suzuki, N. Kasagi, The development of a high-performance perfluorinated polymer electret and its application to micro power generation, J. Micromech. Microeng. 18 (2008), 104011, https://doi.org/10.1088/0960-1317/18/10/104011.
[22] S. Kim, K. Suzuki, A. Sugie, H. Yoshida, M. Yoshida, Y. Suzuki, Effect of end group of amorphous perfluoro-polymer electrets on electron trapping, Sci. Technol. Adv. Mater. 19 (2018) 486–494, https://doi.org/10.1080/14686996.2018.1477395.
[23] D.R. Lamb, Some electrical properties of the silicon-silicon dioxide system, Thin Solid Films 5 (1970) 247–276, https://doi.org/10.1016/0040-6090(70)90096-9.
[24] L. Medda, M. Monduzzi, A. Salis, The molecular motion of bovine serum albumin under physiological conditions is ion specific, Chem. Commun. 51 (2015) 6663–6666, https://doi.org/10.1039/C5CC01538C.